




A Hessian Regularized Nonlinear Time Series Model

Jie Chen & Xiaoming Huo


To cite this article: Jie Chen & Xiaoming Huo (2009) A Hessian Regularized Nonlinear Time Series Model, Journal of Computational and Graphical Statistics, 18:3, 694-716, DOI: [10.1198/jcgs.2009.08040](https://doi.org/10.1198/jcgs.2009.08040)

To link to this article: <https://doi.org/10.1198/jcgs.2009.08040>

 View supplementary material 

 Published online: 01 Jan 2012.

 Submit your article to this journal 

 Article views: 60

 View related articles 



A Hessian Regularized Nonlinear Time Series Model

Jie CHEN and Xiaoming HUO

We introduce a nonparametric nonlinear time series model. The novel idea is to fit a model via penalization, where the penalty term is an unbiased estimator of the integrated Hessian of the underlying function. The underlying model assumption is very general: it has Hessian almost everywhere in its domain. Numerical experiments demonstrate that our model has better predictive power: if the underlying model complies with an existing parametric/semiparametric form (e.g., a threshold autoregressive model (TAR), an additive autoregressive model (AAR), or a functional coefficient autoregressive model (FAR)), our model performs comparably; if the underlying model does *not* comply with any preexisting form, our model outperforms in nearly all simulations. We name our model a Hessian regularized nonlinear model for time series (HRM). We conjecture on theoretical properties and use simulations to verify. Our method can be viewed as a way to generalize splines to high dimensions (when the number of variates is more than three), under which an analogous analytical derivation cannot work due to the curse of dimensionality. Supplemental materials are provided, and will help readers reproduce all results in the article.

Key Words: Additive autoregressive (AAR); Functional coefficient autoregressive (FAR); Nearest neighbors; Penalization estimator; Regularization; Splines; Threshold autoregressive (TAR).

1. INTRODUCTION

In time series analysis, the concepts of autoregressive (AR), moving average (MA), and their combination (ARIMA models) are classical. These models are linear, or linear after a prespecified transform (like exponential). In the past few decades, nonlinear models have been successfully developed and tested. Some works that have been influential include the threshold autoregressive model (TAR) (Tong 1990), additive autoregressive model (AAR) (Hastie and Tibshirani 1990), multivariate local polynomial regression model (Cleveland

Dr. Jie Chen is Technical Member, Bank of America, Charlotte, NC 28255 (E-mail: jiechen2004@gmail.com). Xiaoming Huo is Professor, Georgia Institute of Technology, School of Industrial and Systems Engineering, Atlanta, GA 30332 (E-mail: xiaoming@isye.gatech.edu, www.isye.gatech.edu/~xiaoming).

© 2009 American Statistical Association, Institute of Mathematical Statistics,
and Interface Foundation of North America

Journal of Computational and Graphical Statistics, Volume 18, Number 3, Pages 694–716
DOI: 10.1198/jcgs.2009.08040

1979, 1988; Fan and Gijbels 1996), functional coefficient autoregressive model (Chen and Tsay 1993) and its adaptive version (FAR) (Cai, Fan, and Yao 2000; Fan, Yao, and Cai 2003), among many others. Fan and Yao (2003) provided an excellent contemporary overview. These developments have significantly broadened our modeling capability in time series. However, they still rely on particular assumptions of the functional form. For example, in TAR, the model is assumed to be piecewise linear. In AAR, the underlying model is an additive function. In FAR, the linear combination formulation under an autoregressive framework is preserved, whereas the coefficients are relaxed to be functions of specific types; for example, in the work of Chen and Tsay (1993), they are functions of one covariate, whereas in the work of Fan, Yao, and Cai (2003), they are functions of a unique linear transform of all covariates. These preassumptions potentially raise confusion in practice and leave users pondering which model should be used. The number of proposed models and the foreseeable possibility of many other alternative models also raise the question: is there an approach that unifies them? It is desirable to have an approach that is relatively free from formulational assumptions.

This article introduces a numerical method which only requires the underlying model function to have the Hessian almost everywhere. We consider a penalized model fitting, the objective function being a goodness-of-fit measure (which is also known as the residual sum of squares) plus a penalty term multiplied by an algorithmic parameter (λ). The penalty function is an unbiased estimator of the integrated Hessian of the underlying function. A numerical solution is developed. It is shown that the solution can be given in a closed form; hence implementation is convenient. The novel Hessian estimator utilizes the nearest-neighbors approach and makes no assumption on the model formulation in advance.

In simulations, we compare our approach with other models and obtain appealing results. When the underlying model complies with one existing form (e.g., a TAR model), our method performs comparably. When the underlying model deviates from existing forms, our method consistently outperforms.

Our philosophical starting point is the smoothing spline. Our approach can be considered as a way to generalize smoothing splines to high dimensions. To be more specific, we bring in the formulation. Consider a univariate time series $X_1, X_2, \dots, X_n, \dots, n \geq 1$. A nonlinear data generation mechanism can be written as

$$X_t = f(X_{t-1}, \dots, X_{t-p}) + \varepsilon_t \quad (1.1)$$

for $p + 1 \leq t \leq n$, and iid ε_t 's. Function f has p variables. We assume that f has square integrable second partial derivatives. To simplify the notation, denote $\mathbf{Z}_{t-1} = (X_{t-1}, \dots, X_{t-p})^T \in \mathbb{R}^p$; vector $\mathbf{z} = (z_1, \dots, z_p)^T \in \mathbb{R}^p$ is a generic p -dimensional vector. Let $f_{ij}(\mathbf{z}) = \frac{\partial^2 f(\mathbf{z})}{\partial z_i \partial z_j}$. Recall the integrated Hessian of function f is defined as

$$\mathcal{H}f = \int_{\Omega} \sum_{i,j} |f_{ij}(\mathbf{z})|^2 d\mathbf{z},$$

where subset $\Omega \subset \mathbb{R}^p$ is the support of function f . Because f has square integrable second derivatives, we must have $\mathcal{H}f < \infty$. It is evident that formula (1.1) encompasses many nonlinear time series models. For technical reasons, we assume that $\Omega (\subset \mathbb{R}^p)$ is compact.

Define a functional class: $\mathcal{F} = \{f : \mathcal{H}f < \infty, \text{ and support } f \subset \Omega\}$. A major approach in nonparametric estimation is to consider \hat{f} that is the minimizer to the following problem:

$$\min_{f \in \mathcal{F}} \sum_{t=p+1}^N [X_t - f(\mathbf{Z}_{t-1})]^2 + \lambda \mathcal{H}f. \quad (1.2)$$

Function $\mathcal{H}f$ is called the “bending energy” in deriving the thin-plate spline (Wahba 1990). Note that if $p = 1$, then the minimizer of (1.2) is the natural cubic spline, whose knots are at \mathbf{Z}_t ’s, $p \leq t \leq n - 1$. If $p = 2$ or 3, the solution to (1.2) is the thin-plate spline (Wahba 1990). Unfortunately when $p \geq 4$, the above problem is not well defined (Green and Silverman 1994, sec. 7.9). Hence for $p > 3$, high-dimensional splines cannot be derived by adopting the formulation (1.2).

Our proposed model—Hessian regularized nonlinear time series model (HRM)—uses a surrogate penalty function in (1.2). In a nutshell, the new penalty function is a sum of estimated Hessian at observed points. At each point, the nearest neighbors are utilized, and the pointwise estimate is the Frobenius norm of the least squares estimate of the Hessian (which is a matrix). At this point, theoretical consistency of the numerical approach remains a conjecture. However, simulations provide strong evidence that the consistency holds with significant generality. By considering special cases, some speculative analysis is provided to demonstrate the theoretical derivation that may take place. A full-scale proof seems to be too complex to be accommodated here and is relegated to a future publication. Most importantly, simulations demonstrate the advantage of our method to existing state-of-the-art nonlinear models. The choice of the algorithmic parameter λ is studied. We found that the generalized cross-validation principle can be adopted successfully.

Due to space, a discussion regarding how to realize fast computing is posted in an online report (Chen and Huo 2007, sec. 5), which is freely downloadable. A speculative description of a formal proof of convergence is included in the same report (Chen and Huo 2007, sec. 3.2) as well.

The rest of this article is organized as follows. Section 2 derives a numerical approximation to the functional, given that an analytical solution is not available. Section 3 derives a theorem that reveals some conditions under which our proposed method should work. Section 4 discusses issues related to how to choose an optimal value of λ . Section 5 presents numerical results of some simulations and real data analysis. Discussion and concluding remarks are in Section 6.

2. NUMERICAL APPROXIMATION TO HESSIAN

We propose a numerical approach that emulates problem (1.2). The key idea is to introduce a least squares estimator of the Hessian matrix $\mathcal{H}f(\mathbf{Z}_{t-1})$ at locations \mathbf{Z}_{t-1} , $t = p + 1, p + 2, \dots, n$.

Because \mathbf{Z}_t ’s are random variables, we slightly modify the original Hessian functional $\mathcal{H}f$, so that the density function of \mathbf{Z}_t ’s can be involved. The new Hessian functional is

$$\int_{\Omega} \sum_{i,j} |f_{ij}(\mathbf{z})|^2 g(\mathbf{z}) d\mathbf{z}, \quad (2.1)$$

where $g(\mathbf{z})$ is the density function of \mathbf{z} . Actually, $\mathcal{H}f$ is a special case of (2.1), if \mathbf{z} is uniformly distributed. The objective function (1.2) becomes

$$\min_{f \in \mathcal{F}} \sum_{t=p+1}^N [X_t - f(\mathbf{Z}_{t-1})]^2 + \lambda \int_{\Omega} \sum_{i,j} |f_{ij}(\mathbf{z})|^2 g(\mathbf{z}) d\mathbf{z}. \quad (2.2)$$

An unbiased estimator of functional (2.1) is $\frac{1}{n-p} \sum_{t=p+1}^n \|\mathcal{H}f(\mathbf{Z}_{t-1})\|_F^2$, where $\|\cdot\|_F$ denotes the Frobenius norm (i.e., Euclidean norm) of a matrix. A numerical approximation of problem (2.2) is

$$\min_{f \in \mathcal{F}} \sum_{t=p+1}^N [X_t - f(\mathbf{Z}_{t-1})]^2 + \lambda \sum_{t=p+1}^n \|\mathcal{H}f(\mathbf{Z}_{t-1})\|_F^2. \quad (2.3)$$

2.1 LOCAL LEAST SQUARES ESTIMATE

Now we consider an estimate of functional $\|\mathcal{H}f(\mathbf{Z}_{t-1})\|_F^2$. Recall we have

$$\mathbf{Z}_{t-1} = (X_{t-1}, \dots, X_{t-p})^T \in \mathbb{R}^p.$$

Consider set $\mathcal{V} = \{\mathbf{Z}_{t-1}, p+1 \leq t \leq n\}$ a collection of $(n-p)$ p -dimensional vectors. Assume $\mathbf{V}_0 = \mathbf{Z}_{t-1}$, for $p+1 \leq t \leq n$. Let $\mathbf{V}_i, i = 1, 2, \dots, k$, denote the k ($k \geq 1$) nearest neighbors of \mathbf{V}_0 , whereas $\mathbf{V}_i \in \mathcal{V}$. Let $\bar{\mathbf{V}} = \frac{1}{k+1} \sum_{i=0}^k \mathbf{V}_i$, that is, $\bar{\mathbf{V}}$ is the average of the $k+1$ vectors. A Taylor expansion at point $\bar{\mathbf{V}}$ generates the following approximation:

$$\begin{aligned} f(\mathbf{V}_i) &\approx f(\bar{\mathbf{V}}) + (\mathbf{V}_i - \bar{\mathbf{V}})^T \mathcal{J}f(\bar{\mathbf{V}}) \\ &\quad + \frac{1}{2} (\mathbf{V}_i - \bar{\mathbf{V}})^T \mathcal{H}f(\bar{\mathbf{V}}) (\mathbf{V}_i - \bar{\mathbf{V}}), \quad i = 0, 1, \dots, k, \end{aligned}$$

where $f(\bar{\mathbf{V}})$ is the value of function f at location $\bar{\mathbf{V}}$, $\mathcal{J}f(\bar{\mathbf{V}})$ is the Jacobian at $\bar{\mathbf{V}}$, and $\mathcal{H}f(\bar{\mathbf{V}})$ is the Hessian matrix at $\bar{\mathbf{V}}$. Note we have $\mathcal{J}f(\bar{\mathbf{V}}) \in \mathbb{R}^p$ and $\mathcal{H}f(\bar{\mathbf{V}}) \in \mathbb{R}^{p \times p}$.

If f is analytical, then the above approximation is close. A matrix version of the above approximation is

$$\mathbf{f}^* \approx \mathbf{1}_{k+1} \cdot c + \mathbf{V} \cdot \mathbf{J} + \frac{1}{2} \mathbf{C} \cdot \mathbf{H}, \quad (2.4)$$

where

$$\begin{aligned} \mathbf{f}^* &= (f(\mathbf{V}_0), f(\mathbf{V}_1), \dots, f(\mathbf{V}_k))^T \in \mathbb{R}^{k+1}, \\ \mathbf{1}_{k+1} &= (1, \dots, 1)^T \in \mathbb{R}^{k+1}, \end{aligned}$$

c is a constant; the i th ($1 \leq i \leq k+1$) row of matrix \mathbf{V} , $\mathbf{V} \in \mathbb{R}^{(k+1) \times p}$, is $(\mathbf{V}_{i-1} - \bar{\mathbf{V}})^T$; vector $\mathbf{J} \in \mathbb{R}^p$ is the Jacobian ($J_i = f_i(\bar{\mathbf{V}})$) at $\bar{\mathbf{V}}$. The i th row of matrix \mathbf{C} , $\mathbf{C} \in \mathbb{R}^{(k+1) \times (p^2+p)/2}$, is $\mathcal{V}_1[(\mathbf{V}_i - \bar{\mathbf{V}})(\mathbf{V}_i - \bar{\mathbf{V}})^T]$, where for an arbitrary column vector $\mathbf{x} = (x_1, x_2, \dots, x_p)^T$, we define $\mathcal{V}_1[\mathbf{x} \cdot \mathbf{x}^T] = (x_1^2, x_2^2, \dots, x_p^2, \sqrt{2}x_1x_2, \dots, \sqrt{2}x_1x_p, \sqrt{2}x_2x_3, \dots, \sqrt{2}x_2x_p, \dots, \sqrt{2}x_{p-1}x_p) \in \mathbb{R}^{(p^2+p)/2}$. Vector \mathbf{H} is a vectorization with respect to the Hessian matrix at $\bar{\mathbf{V}}$, after eliminating identical entries: $\mathbf{H} = \mathcal{V}_2[\mathcal{H}f(\bar{\mathbf{V}})]$, where for a symmetric matrix $\mathbf{S} = (S_{ij}) \in \mathbb{R}^{p \times p}$, we have $\mathcal{V}_2[\mathbf{S}] = (S_{11}, S_{22}, \dots, S_{pp}, \sqrt{2}S_{12}, \sqrt{2}S_{13}, \dots, \sqrt{2}S_{1p}, \sqrt{2}S_{23}, \dots, \sqrt{2}S_{2p}, \dots, \sqrt{2}S_{p-1,p})^T$. It is a standard exercise to verify that $\mathbf{1}^T \mathbf{V} = \mathbf{0}$.

A partial implementation of QR-decomposition (via, e.g., a modified Gram–Schmidt algorithm) can produce

$$[\mathbf{1}_{k+1} \quad \mathbf{V} \quad \frac{1}{2}\mathbf{C}] = [\mathbf{Q}_1 \quad \mathbf{Q}_2] \begin{bmatrix} \mathbf{R}_{11} & \mathbf{R}_{12} \\ \mathbf{0} & \mathbf{I}_{(p^2+p)/2} \end{bmatrix}, \quad (2.5)$$

where columns of $\mathbf{Q}_1 \in \mathbb{R}^{(k+1) \times (p+1)}$ are orthonormal ($\mathbf{Q}_1^T \mathbf{Q}_1 = \mathbf{I}_{p+1}$), and columns of $\mathbf{Q}_2 \in \mathbb{R}^{(k+1) \times (p^2+p)/2}$ are orthogonal to the columns of \mathbf{Q}_1 (i.e., $\mathbf{Q}_2^T \mathbf{Q}_1 = \mathbf{0}$).

From (2.4), we have

$$\begin{aligned} \mathbf{Q}_2^T \mathbf{f}^* &= (\mathbf{0} \quad \mathbf{Q}_2^T \mathbf{Q}_2) \begin{bmatrix} \mathbf{R}_{11} & \mathbf{R}_{12} \\ \mathbf{0} & \mathbf{I}_{(p^2+p)/2} \end{bmatrix} \begin{bmatrix} c \\ \mathbf{J} \\ \mathbf{H} \end{bmatrix} \\ &= \mathbf{Q}_2^T \mathbf{Q}_2 \mathbf{H}. \end{aligned}$$

Hence, a least squares estimator of \mathbf{H} is

$$\hat{\mathbf{H}} = (\mathbf{Q}_2^T \mathbf{Q}_2)^+ \mathbf{Q}_2^T \mathbf{f}^*,$$

where $(\cdot)^+$ denotes a pseudo-inverse of a matrix.

For the local Hessian matrix, we have

$$\begin{aligned} \|\hat{\mathcal{H}}f(\mathbf{Z}_{t-1})\|_F^2 &= \|\hat{\mathbf{H}}\|_2^2 = \hat{\mathbf{H}}^T \hat{\mathbf{H}} \\ &= (\mathbf{f}^*)^T \mathbf{Q}_2 (\mathbf{Q}_2^T \mathbf{Q}_2)^+ (\mathbf{Q}_2^T \mathbf{Q}_2)^+ \mathbf{Q}_2^T \mathbf{f}^*. \end{aligned}$$

2.2 GLOBAL ESTIMATION AND A CLOSE FORM SOLUTION

Now we consider the objective function in (2.3). We will show that it is a quadratic form. To construct the matrix form of (2.3), we introduce the following notation:

$$\mathbf{K}_{t-1} = \mathbf{Q}_2 (\mathbf{Q}_2^T \mathbf{Q}_2)^+ (\mathbf{Q}_2^T \mathbf{Q}_2)^+ \mathbf{Q}_2^T.$$

We also bring in a selection matrix \mathbf{S}_{t-1} , $p+1 \leq t \leq n$. Matrix \mathbf{S}_{t-1} , $\mathbf{S}_{t-1} \in \mathbb{R}^{(k+1) \times (n-p)}$, is made by two possible components: 0 and 1. For $\mathbf{V}_0, \mathbf{V}_1, \dots, \mathbf{V}_k$ and $\mathbf{Z}_p, \dots, \mathbf{Z}_{n-1}$ that are defined previously, \mathbf{S}_{t-1} satisfies

$$(\mathbf{V}_0, \mathbf{V}_1, \dots, \mathbf{V}_k) = (\mathbf{Z}_p, \mathbf{Z}_{p+1}, \dots, \mathbf{Z}_{n-1}) \mathbf{S}_{t-1}^T \quad \forall t.$$

Apparently we have $\mathbf{f}^* = \mathbf{S}_{t-1} \mathbf{f}$, where $\mathbf{f} = (f(\mathbf{Z}_p), f(\mathbf{Z}_{p+1}), \dots, f(\mathbf{Z}_{n-1}))^T$. We have

$$\sum_{t=p+1}^n \|\hat{\mathcal{H}}f(\mathbf{Z}_{t-1})\|_F^2 = \sum_{t=p}^{n-1} (\mathbf{f}^T \mathbf{S}_t^T \mathbf{K}_t \mathbf{S}_t \mathbf{f}).$$

Let

$$\mathbf{M} = (\mathbf{S}_p^T, \dots, \mathbf{S}_{n-1}^T) \text{diag}\{\mathbf{K}_p, \mathbf{K}_{p+1}, \dots, \mathbf{K}_{n-1}\} \begin{pmatrix} \mathbf{S}_p \\ \vdots \\ \mathbf{S}_{n-1} \end{pmatrix};$$

we have

$$\sum_{t=p+1}^n \|\hat{\mathcal{H}}f(\mathbf{Z}_{t-1})\|_F^2 = \mathbf{f}^T \mathbf{M} \mathbf{f},$$

which is a quadratic function of \mathbf{f} .

Problem (2.3) becomes

$$\min_{\mathbf{f}} \|\mathbf{Y} - \mathbf{f}\|_2^2 + \lambda \mathbf{f}^T \mathbf{M} \mathbf{f},$$

where we have variable $\mathbf{f} \in \mathbb{R}^{n-p}$, vector $\mathbf{Y} = (X_{p+1}, \dots, X_n)^T \in \mathbb{R}^{n-p}$, and matrix \mathbf{M} defined previously. The estimator of \mathbf{f} becomes

$$\hat{\mathbf{f}} = (\mathbf{I}_{n-p} + \lambda \cdot \mathbf{M})^{-1} \cdot \mathbf{Y}. \quad (2.6)$$

In numerical implementation, it may be faster to treat $\hat{\mathbf{f}}$ as a solution to the following system of linear equations: $(\mathbf{I}_{n-p} + \lambda \cdot \mathbf{M}) \cdot \hat{\mathbf{f}} = \mathbf{Y}$.

2.3 NULL SPACE OF MATRIX \mathbf{M}

The estimator in (2.6) requires inverting an $(n-p) \times (n-p)$ matrix, which can be challenging. It is easy to verify that matrix \mathbf{M} is positive-semidefinite. Moreover, matrix \mathbf{M} has eigenvalue 0, whose multiplicity is at least $p+1$, conditioning that the following matrix is of full column rank:

$$\begin{pmatrix} 1 & \mathbf{Z}_p^T \\ \vdots & \vdots \\ 1 & \mathbf{Z}_{n-1}^T \end{pmatrix}.$$

As a matter of fact, every column of the above matrix solves the equation $\mathbf{M} \cdot \mathbf{x} = 0$.

2.4 PREDICTION

We estimate $f(\mathbf{Z})$ at a new point $\mathbf{Z} \in \mathbb{R}^p$. First we identify the $k+1$ ($k \geq 1$) nearest neighbors of \mathbf{Z} for the vectors in the set \mathcal{V} . The reason for choosing the $k+1$ instead of k nearest neighbors is that we want a similar expression in the prediction step as in the estimation step. Recall \mathcal{V} contains all the p -dimensional vectors generated by a scanning window going through the time series. Without loss of generality, let $\mathbf{V}_1, \mathbf{V}_2, \dots, \mathbf{V}_{k+1}$ denote the $k+1$ nearest neighbors. Let $\bar{\mathbf{V}}$ denote the average: $\bar{\mathbf{V}} = \frac{1}{k+1} \sum_{i=1}^{k+1} \mathbf{V}_i$. Recall $\mathcal{J}f(\bar{\mathbf{V}})$ denotes the Jacobian at $\bar{\mathbf{V}}$, and $\mathcal{H}f(\bar{\mathbf{V}})$ denotes the Hessian matrix at $\bar{\mathbf{V}}$. A second-order approximation via Taylor expansion at point $\bar{\mathbf{V}}$ yields

$$f(\mathbf{V}_i) - f(\bar{\mathbf{V}}) = (\mathbf{V}_i - \bar{\mathbf{V}})^T \mathcal{J}f(\bar{\mathbf{V}}) + \frac{1}{2} (\mathbf{V}_i - \bar{\mathbf{V}})^T \mathcal{H}f(\bar{\mathbf{V}}) (\mathbf{V}_i - \bar{\mathbf{V}}).$$

Recall $\hat{f}(\mathbf{V}_1), \dots, \hat{f}(\mathbf{V}_{k+1})$ are the fitted values at $\mathbf{V}_1, \dots, \mathbf{V}_{k+1}$. Similarly to the analysis in establishing the least squares estimators for Hessian, we have the following equation:

$$\begin{pmatrix} \hat{f}(\mathbf{V}_1) \\ \vdots \\ \hat{f}(\mathbf{V}_{k+1}) \end{pmatrix} = \mathbf{1}_{k+1} f(\bar{\mathbf{V}}) + \begin{pmatrix} (\mathbf{V}_1 - \bar{\mathbf{V}})^T \\ \vdots \\ (\mathbf{V}_{k+1} - \bar{\mathbf{V}})^T \end{pmatrix} \mathcal{J}f(\bar{\mathbf{V}}) + \frac{1}{2} \begin{pmatrix} \mathcal{V}_1[(\mathbf{V}_1 - \bar{\mathbf{V}})(\mathbf{V}_1 - \bar{\mathbf{V}})^T] \\ \vdots \\ \mathcal{V}_1[(\mathbf{V}_{k+1} - \bar{\mathbf{V}})(\mathbf{V}_{k+1} - \bar{\mathbf{V}})^T] \end{pmatrix} \mathcal{V}_2[\mathcal{H}f(\bar{\mathbf{V}})], \quad (2.7)$$

where vectorization operators $\mathcal{V}_1(\cdot)$ and $\mathcal{V}_2(\cdot)$ have been defined previously. Note $f(\bar{\mathbf{V}})$ is a scalar, vector $\mathcal{J}f(\bar{\mathbf{V}})$ is p -dimensional, and matrix $\mathcal{H}f(\bar{\mathbf{V}})$ contains $p(p+1)/2$ unknown variables. If we have

$$k \geq p + \frac{p(p+1)}{2} = \frac{1}{2}(p+1)(p+2),$$

then least squares estimators can be established for $f(\bar{\mathbf{V}})$, $\mathcal{J}f(\bar{\mathbf{V}})$, and $\mathcal{H}f(\bar{\mathbf{V}})$ on the right side of (2.7). Hence, an estimated value of $f(\cdot)$ at \mathbf{Z} is

$$\hat{f}(\mathbf{Z}) = \hat{f}(\bar{\mathbf{V}}) + (\mathbf{Z} - \bar{\mathbf{V}})^T \hat{\mathcal{J}}f(\bar{\mathbf{V}}) + \frac{1}{2}(\mathbf{Z} - \bar{\mathbf{V}})^T \hat{\mathcal{H}}f(\bar{\mathbf{V}})(\mathbf{Z} - \bar{\mathbf{V}}). \quad (2.8)$$

A variation of the above is to ignore the quadratic terms on the right sides of (2.7) and (2.8). Hence instead of a quadratic prediction, we adopt a linear prediction, where the first-order approximation via Taylor expansion is applied, and the least squares estimators are established for $f(\bar{\mathbf{V}})$ and $\mathcal{J}f(\bar{\mathbf{V}})$. Thus, the prediction of $f(\cdot)$ at \mathbf{Z} is

$$\hat{f}(\mathbf{Z}) = \hat{f}(\bar{\mathbf{V}}) + (\mathbf{Z} - \bar{\mathbf{V}})^T \hat{\mathcal{J}}f(\bar{\mathbf{V}}).$$

The simulation results show that the linear prediction is more robust than the quadratic prediction. This probably is because the second partial derivatives are estimated in (2.8). The estimation error outruns the benefit of a more complex model. Thus, in our numerical experiments, only the linear prediction is utilized.

3. WHEN DOES THE NUMERICAL APPROACH WORK?

We have introduced a numerical approximation to (2.2). Given an underlying function f that is smooth enough, when will the estimator $\hat{\mathbf{f}}$ converge to the underlying function? In this section, we study the quantity $\|\hat{\mathbf{f}}_n - \mathbf{f}\|_2^2/n$, where $\hat{\mathbf{f}}_n$ is identical to $\hat{\mathbf{f}}$ but with a subscript to indicate the length of the time series n , and vector \mathbf{f} is the true value of the function at \mathbf{Z}_t 's. We conjecture that $\|\hat{\mathbf{f}}_n - \mathbf{f}\|_2^2/n \rightarrow 0$ under certain conditions that only depend on matrix \mathbf{M} and the underlying function $f(\cdot)$. These conditions can be verified numerically and hence can be checked in simulations. Our conditions are analogous to the conditions for Sobolev space, which has played an important role in determining the optimal rate of estimation within a certain functional class (Johnstone 2004).

We establish an upper bound for the error ($\|\hat{\mathbf{f}}_n - \mathbf{f}\|_2^2$). Recall

$$\hat{\mathbf{f}}_n = (\mathbf{I}_{n-p} + \lambda_n \mathbf{M})^{-1} \mathbf{Y}.$$

Consequently, we have

$$\hat{\mathbf{f}}_n - \mathbf{f} = (\mathbf{I} + \lambda_n \mathbf{M})^{-1} \mathbf{f} - \mathbf{f} + (\mathbf{I} + \lambda_n \mathbf{M})^{-1} \varepsilon,$$

where $\varepsilon = (\varepsilon_{p+1}, \dots, \varepsilon_n)^T$.

Let $\mathbf{M} = \mathbf{U}^T \mathbf{D} \mathbf{U}$ be the eigenvalue decomposition of matrix \mathbf{M} . Denote $\mathbf{D} = \text{diag}\{d_1, \dots, d_{n-p}\}$. Let $f'_i = (\mathbf{U}\mathbf{f})_i$ and $\varepsilon'_i = (\mathbf{U}\varepsilon)_i$.

Lemma 1. *There exists a constant c_n (e.g., $c_n = 2 \log n$; Johnstone 2004), such that for $\varepsilon_i \stackrel{iid}{\sim} N(0, \sigma^2)$,*

$$\Pr\{|\varepsilon'_i|^2 < c_n \sigma^2, \forall i\} \rightarrow 1, \quad \text{as } n \rightarrow \infty.$$

The above is a well-known property of normally distributed random variables.

We have the following inequality, with high probability:

$$\begin{aligned} \frac{1}{2} \|\hat{\mathbf{f}}_n - \mathbf{f}\|_2^2 &\leq \sum_{i=1}^{n-p} \frac{(\lambda_n d_i)^2 (f'_i)^2 + (\varepsilon'_i)^2}{(1 + \lambda_n d_i)^2} \\ &\leq \sum_{i=1}^{n-p} \frac{(\lambda_n d_i)^2 (f'_i)^2 + c_n \sigma^2}{(1 + \lambda_n d_i)^2}. \end{aligned}$$

The last inequality utilizes the preceding lemma. We consider a function: for $\alpha \geq 0$,

$$g(\alpha) = \frac{\alpha^2 (f'_i)^2 + c_n \sigma^2}{(1 + \alpha)^2}.$$

The following can be verified through elementary calculation:

1. $g(0) = c_n \sigma^2$, $g(\infty) = (f'_i)^2$.
2. When $0 < \alpha < \frac{c_n \sigma^2}{(f'_i)^2}$, we have $g'(\alpha) < 0$; when $\alpha > \frac{c_n \sigma^2}{(f'_i)^2}$, we have $g'(\alpha) > 0$.
3. The minimum point is $g(\frac{c_n \sigma^2}{(f'_i)^2}) = \frac{(c_n \sigma^2)(f'_i)^2}{(f'_i)^2 + c_n \sigma^2}$.
4. If $(f'_i)^2 < c_n \sigma^2$ and $\alpha > \frac{1}{\gamma} \frac{c_n \sigma^2}{(f'_i)^2}$, where $\gamma \geq 1$, we have $g(\alpha) < \gamma (f'_i)^2$.
5. If $c_n \sigma^2 < (f'_i)^2$ and $\alpha < \gamma \frac{c_n \sigma^2}{(f'_i)^2}$, where $\gamma \geq 1$, we have $g(\alpha) < \gamma \cdot c_n \sigma^2$.

Consider two quantities:

$$\begin{aligned} a_n &= \max_i \left\{ \frac{c_n \sigma^2}{(f'_i)^2} \cdot \frac{1}{d_i} : \text{for } i \text{ such that } (f'_i)^2 < c_n \sigma^2 \right\}, \\ b_n &= \min_i \left\{ \frac{c_n \sigma^2}{(f'_i)^2} \cdot \frac{1}{d_i} : \text{for } i \text{ such that } (f'_i)^2 > c_n \sigma^2 \right\}. \end{aligned}$$

It will not be interesting if $a_n \leq b_n$. We suppose that

$$\gamma_n = \sqrt{\frac{a_n}{b_n}} \geq 1.$$

We pick $\lambda_n = \frac{a_n}{\gamma_n} = b_n \cdot \gamma_n = \sqrt{a_n b_n}$ and derive the following main result.

Theorem 1. For the aforementioned λ_n , we have, with high probability,

$$\frac{1}{2} \|\hat{\mathbf{f}}_n - \mathbf{f}\|_2^2 \leq \gamma_n \cdot \sum_{i=1}^{n-p} \min[(f'_i)^2, c_n \sigma^2].$$

The proof is an application of the preceding analysis. If the right side converges to a finite number, then convergence is achieved. Section 5.1 provides some examples where $\sum_{i=1}^{n-p} \min[(f'_i)^2, c_n \sigma^2]/n$ does decay with the increasing n . It is still an open question whether γ_n remains a constant.

In simulated examples, in almost all the cases, we observe that the sequence $|f'_i|$ (after being sorted in a decreasing order) decays like an inverse polynomial (i.e., $x^{-\beta}$ for $\beta > 0$; in fact, in most cases, we observe that $\beta > 1/2$). From the above theorem, our estimator will converge to the truth in those situations: the right side of the above inequality is bounded, hence we have $\|\hat{\mathbf{f}}_n - \mathbf{f}\|_2^2/n \rightarrow 0$ as $n \rightarrow \infty$. The speculation on a formal proof of convergence is in the work of [Chen and Huo \(2007, sec. 3.2\)](#); it also presents a special case under which the derived upper bound converges to zero when n goes to infinity. The special case motivates us to believe that the convergence is true in general cases.

4. CHOICE OF PENALTY PARAMETER λ

In Section 3, a theoretical appropriation λ_n is provided. However, in practice, the underlying function $f(\cdot)$ is not available; hence, one cannot utilize the theoretical formula. Generalized cross-validation can be adopted. Consider the generalized cross-validation function $\text{GCV}(\lambda)$:

$$\text{GCV}(\lambda) = \frac{1}{n-p} \sum_{k=p+1}^n \left(\frac{X_k - \hat{f}_\lambda(\mathbf{Z}_{k-1})}{1 - \frac{1}{n-p} \text{Tr}(\mathbf{A}(\lambda))} \right)^2, \quad (4.1)$$

where $\mathbf{A}(\lambda) = (\mathbf{I}_{n-p} + \lambda \mathbf{M})^{-1}$. The optimal value of the penalty parameter λ can be estimated by minimizing the above GCV function. The justification is relatively straightforward and can be found in the work of [Chen \(2007\)](#).

The derivation of the GCV function uses an approximation, because of the numerical approximation of the Hessian functional. The following provides more justification for applying GCV. To facilitate the following analysis, let us recall some notations. The eigenvalue decomposition of matrix \mathbf{M} is $\mathbf{M} = \mathbf{U}^T \mathbf{D} \mathbf{U}$, where $\mathbf{D} = \text{diag}\{d_1, \dots, d_{n-p}\}$, and $0 \leq d_1 \leq d_2 \leq \dots \leq d_{n-p}$. Recall that $\varepsilon'_i = (\mathbf{U}\varepsilon)_i$ and $y'_i = (\mathbf{U}\mathbf{Y})_i$. Note vectors \mathbf{f} , \mathbf{Y} , ε have been used in Section 3. If we know the true value of the function at every point (i.e., \mathbf{f} is known), then the mean squared error as a function of λ is

$$\begin{aligned} \text{MSE}(\lambda) &= \frac{1}{n-p} \|\mathbf{f} - \mathbf{A}(\lambda)\mathbf{Y}\|_2^2 \\ &= \frac{1}{n-p} \|[\mathbf{I} - \mathbf{A}(\lambda)]\mathbf{Y} - \varepsilon\|_2^2 \\ &= \frac{1}{n-p} \{ \|[\mathbf{I} - \mathbf{A}(\lambda)]\mathbf{Y}\|_2^2 + \|\varepsilon\|_2^2 - 2\varepsilon^T [\mathbf{I} - \mathbf{A}(\lambda)]\mathbf{Y} \} \\ &= \frac{1}{n-p} [\lambda^2 h_1(\lambda) + \|\varepsilon\|_2^2 - 2\lambda h_2(\lambda)], \end{aligned} \quad (4.2)$$

where

$$h_1(\lambda) = \sum_i \frac{d_i^2 (y'_i)^2}{(1 + \lambda d_i)^2}$$

and

$$h_2(\lambda) = \sum_i \frac{d_i \cdot \varepsilon'_i \cdot y'_i}{1 + \lambda d_i}.$$

On the other hand, for GCV, we have

$$\text{GCV}(\lambda) = (n - p) \frac{h_1(\lambda)}{[h_3(\lambda)]^2}, \quad (4.3)$$

where

$$h_3(\lambda) = \sum_i \frac{d_i}{1 + \lambda d_i}.$$

Hopefully, one can establish a quantitative connection between the minimizer of (4.2) and the minimizer of (4.3). This article does not pursue this issue further. Note that if factor $\varepsilon'_i \cdot y'_i$ can be treated as a constant, there is a strong similarity between $h_2(\lambda)$ and $h_3(\lambda)$. In simulations, we plot $\text{GCV}(\lambda)$ and $\text{MSE}(\lambda)$ for multiple examples. In almost all the cases, we observe that the minima of the two functions are close. This in some sense validates the use of GCV to choose λ . More details are given in Section 5.2.

5. NUMERICAL EXPERIMENTS

Throughout this section, we consider p to be given. The optimal choice of p for a given dataset can be intricate and is not addressed here. By default, the number of nearest neighbors is set to be $k = 20$, which applies to Sections 5.1–5.3. For the real data experiments in Section 5.4, k is decided by minimizing GCV. We observe that the outcome is insensitive to the value of k , as long as k is close to a reasonable number (such as 20).

5.1 SIMULATIONS REGARDING THE CONVERGENCE THEOREM

The following model is utilized to generate four times series:

$$X_t = f(X_{t-1}, X_{t-2}, X_{t-3}, X_{t-4}) + \varepsilon_t \quad \text{for } t \geq 5,$$

where $\varepsilon_t \stackrel{\text{iid}}{\sim} N(0, \sigma^2)$, and $\sigma = 1$ for the first two time series, $\sigma = 0.2$ for the third time series, and $\sigma = 0.8$ for the last time series. We consider $p = 4$. The function $f(X_{t-1}, X_{t-2}, X_{t-3}, X_{t-4})$ is defined as:

- in the first time series, we have

$$f(x_1, x_2, x_3, x_4) = a_1 + a_2 + a_3 + a_4,$$

where

$$\begin{aligned} a_1 &= -x_2 \exp(-x_2^2/2), \\ a_2 &= \frac{x_1}{1 + x_2^2} \cos(1.5x_2), \\ a_3 &= \frac{4x_3}{1 + 0.8x_3^2}, \\ a_4 &= \frac{\exp(3(x_4 - 2))}{1 + \exp(3(x_4 - 2))}; \end{aligned}$$

- in the second time series, we have

$$f(x_1, x_2, x_3, x_4) = \frac{2x_1}{1 + 0.8x_1^2} - \frac{2x_2}{1 + 0.8x_2^2} + \frac{2x_3}{1 + 0.8x_3^2} - \frac{2x_4}{1 + 0.8x_4^2};$$

- in the third time series, we have

$$f(x_1, x_2, x_3, x_4) = a_1x_1 + a_2x_2 + a_1x_3 + a_2x_4, \quad (5.1)$$

where

$$a_1 = 0.2 + (0.3 + x_1) \exp(-4x_1^2),$$

$$a_2 = -0.4 - (0.7 + 1.3x_1) \exp(-4x_1^2);$$

- in the last time series, we have

$$\begin{aligned} f(x_1, x_2, x_3, x_4) = & \frac{0.25x_4}{1 + 1.2x_1^2} - \frac{0.4x_1}{1 + 0.6x_2^2} + \frac{0.5x_2}{1 + 0.8x_3^2} \\ & - \frac{0.75x_3}{1 + x_4^2} + \frac{\exp(1.5(x_4 - 2))}{1 + \exp(3(x_4 - 2))}. \end{aligned}$$

The simulated time series are in Figures 1 and 2.

For each model, time series with the different lengths ranging from 200 to 3,000 are generated. The increment of the length of time series is 200. Two quantities $\sum_{i=1}^{n-p} \min[(f'_i)^2, c_n \sigma^2]/n$ and $\sum_{i=1}^{n-p} (f'_i)^2/n$ are calculated and plotted for each time series in Figure 3. (In Figure 3, we plot only for the first two cases. Similar pattern is observed in the other two cases. Also in Figure 3, to compare two quantities more clearly, we normalize the two sequences by dividing their maximal values respectively. Without normalization, $\sum_{i=1}^{n-p} \min[(f'_i)^2, c_n \sigma^2]/n$ is always smaller than $\sum_{i=1}^{n-p} (f'_i)^2/n$.) Quantity $\sum_{i=1}^{n-p} (f'_i)^2/n$ fluctuates around a constant for time series of different lengths, whereas quantity $\sum_{i=1}^{n-p} \min[(f'_i)^2, c_n \sigma^2]/n$ decays as the length of the time series increases. The above observation verifies our conjecture: although $\sum_{i=1}^{n-p} (f'_i)^2/n$ tends to be a constant, $\sum_{i=1}^{n-p} \min[(f'_i)^2, c_n \sigma^2]/n$ could have lower order; that is, it is possible that $n^{-1} \gamma_n \sum_{i=1}^{n-p} \min[(f'_i)^2, c_n \sigma^2] \rightarrow 0$.

5.2 ADOPTION OF THE GENERALIZED CROSS-VALIDATION PRINCIPLE

Using simulations of the four time series in the last section, we study the relation between the minimizers of $\text{GCV}(\cdot)$ and $\text{MSE}(\cdot)$. Because the data generation mechanism is known, we can plot $\text{MSE}(\lambda)$ for a range of values for λ . Function $\text{MSE}(\cdot)$ is plotted along with $\text{GCV}(\cdot)$ in Figure 4. (Again, we plot for the first two cases; similar pattern has been observed in the other two cases.) It is evident that the minimizer of GCV also renders a small value of MSE , which can be considered as a validation of using the GCV function to choose an optimal λ . As a matter of fact, the above phenomenon persists for a range of $k: 20 \leq k \leq 40$. Such a pattern holds consistently through different data generation schemes that we have tried, including those to be mentioned. To save space, we do not include all simulation results.

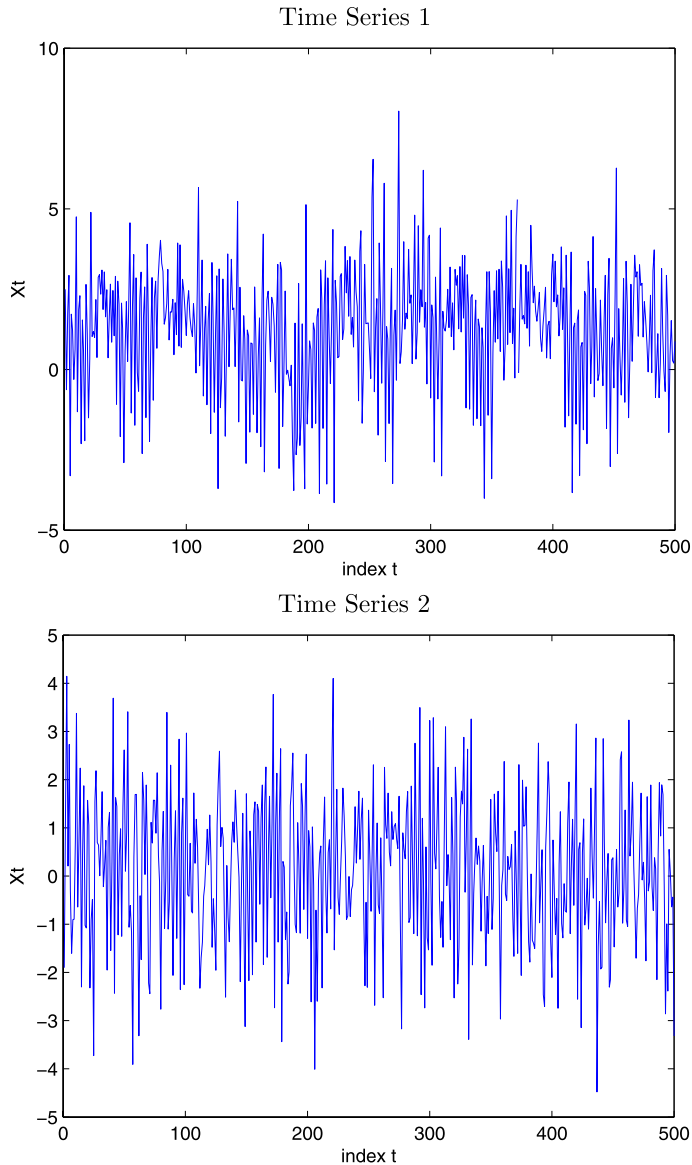


Figure 1. The first two simulated time series with 500 data points. The data generation mechanism is in Section 5.1.

5.3 SYNTHETIC EXAMPLES

This section contains three parts. The first two parts consist of synthetic models, which are chosen from functional coefficient autoregressive model (FAR) and threshold autoregressive model (TAR). The last part consists of two other synthetic models, both of which are nonlinear and do not belong to either the FAR, TAR, or additive autoregressive models (AAR). For each of the models, three types of prediction errors—one-step prediction errors, iterative two-step prediction errors, and direct two-step prediction errors—are com-

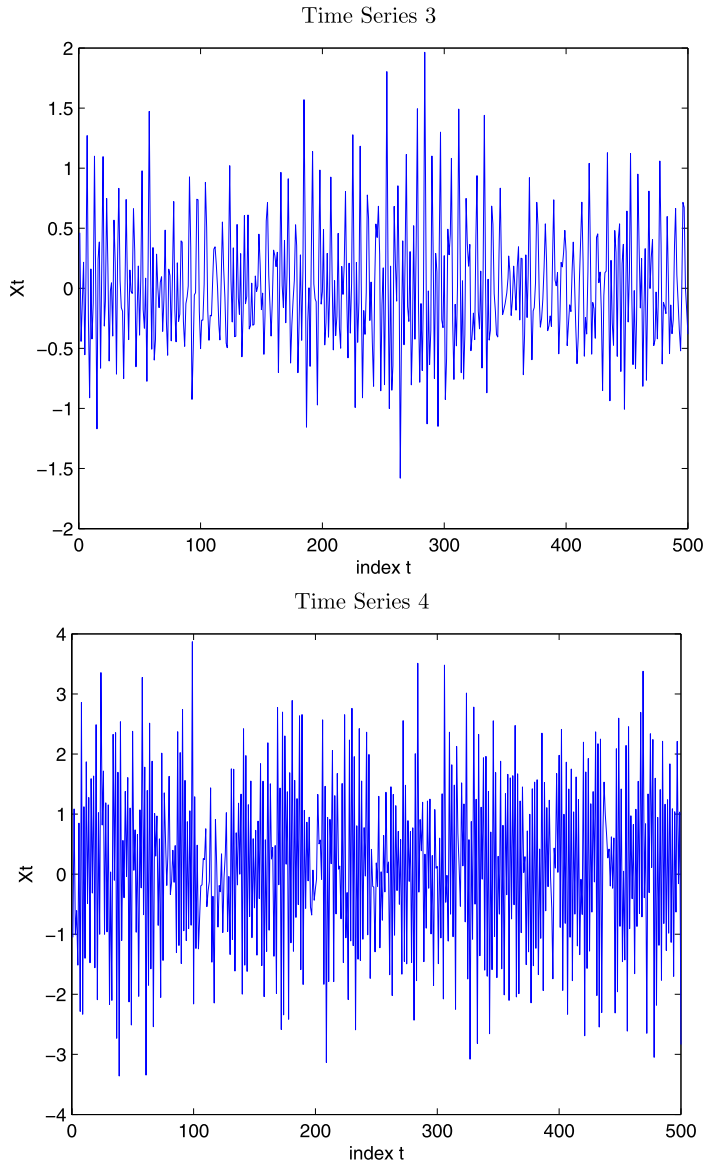


Figure 2. The last two simulated time series with 500 data points. The data generation mechanism is again in Section 5.1.

puted for AAR, FAR, TAR, AR, Loess, Locpoly, and our method. The difference between *iterative* two-step prediction and *direct* two-step prediction can be found in the work of Fan and Yao (2003, sec. 8.3.6). The following is a brief introduction of the models we applied for comparison:

- AAR(p): additive nonlinear autoregressive model with the embedding dimension p . The formula is

$$X_t = f_1(X_{t-1}) + \cdots + f_p(X_{t-p}) + \varepsilon_t.$$

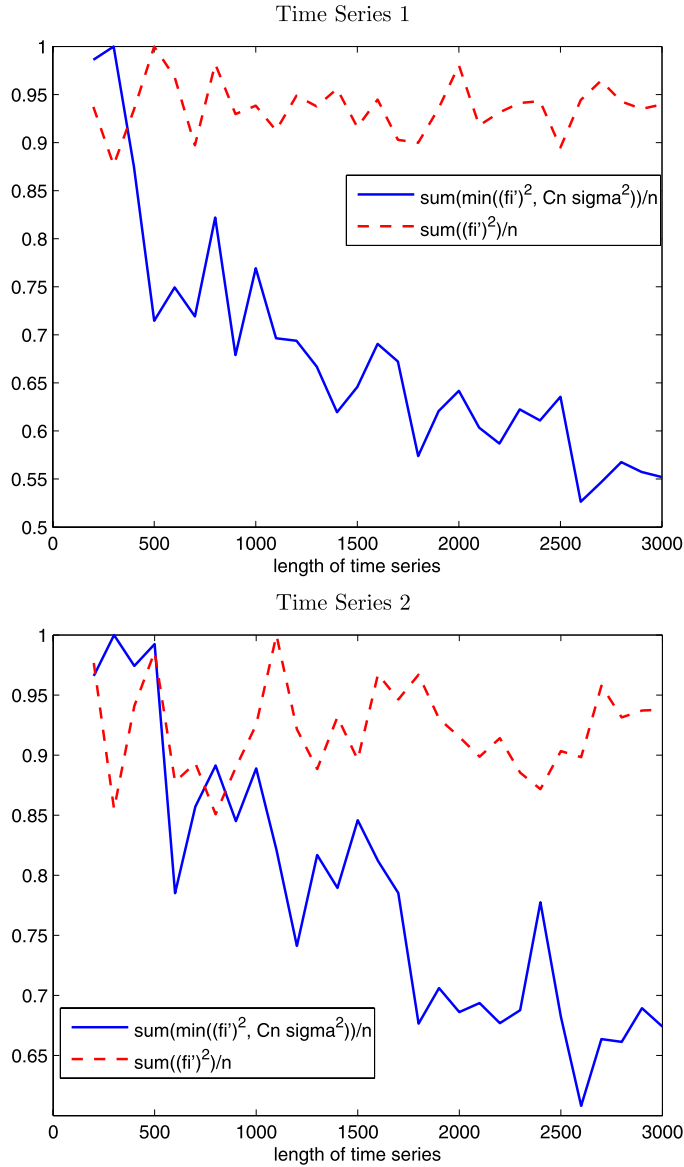


Figure 3. The trend of $\sum_{i=1}^{n-p} \min[(f'_i)^2, c_n \sigma^2]/n$ and $\sum_{i=1}^{n-p} (f'_i)^2/n$ as n increases. The length of time series n ranges from 200 to 3,000.

- FAR(p, d): functional coefficient autoregressive model (Chen and Tsay 1993) with p lags and X_{t-d} being the model-dependent variable (see Fan and Yao 2003, p. 318, for additional details). The formula is

$$X_t = f_1(X_{t-d})X_{t-1} + \cdots + f_p(X_{t-d})X_{t-p} + \varepsilon_t.$$

- AR(p): autoregressive model with p lags.

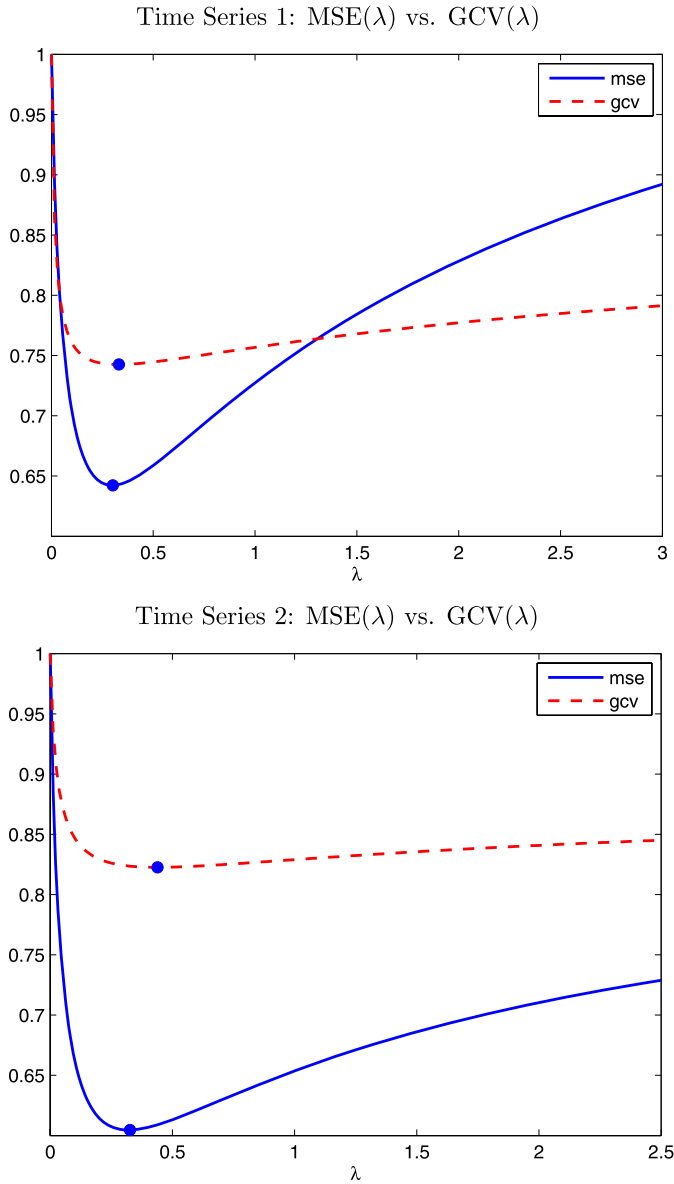


Figure 4. The functions $GCV(\cdot)$ and $MSE(\cdot)$ of the first two time series. The GCV and MSE achieve minima at $(0.3317, 0.3015)$ and $(0.4397, 0.3266)$, respectively. The minima are marked with circles. For comparison, the maximal values of functions GCV and MSE are normalized to 1.

- $TAR(p_1, p_1; d)$: threshold autoregressive model (Tong 1990, sec. 3.3), where p_1 and p_2 are autoregressive orders for low and high regime, respectively, and d is the time delay or time lag for the threshold variable. The formula is

$$X_t = \begin{cases} b_{10} + b_{11}X_{t-1} + \cdots + b_{1p_1}X_{t-p_1} + \varepsilon_t & \text{if } X_{t-d} \leq c \\ b_{20} + b_{21}X_{t-1} + \cdots + b_{2p_2}X_{t-p_2} + \varepsilon_t & \text{if } X_{t-d} > c. \end{cases}$$

- Loess(p) (or Lowess(p)): locally weighted scatterplot smoothing with p covariates (Cleveland 1979, 1988). It is a local polynomial regression with tricubic weighting.
- Locpoly(p): multivariate local polynomial regression with Epanechnikov kernel. p is the number of covariates (Fan and Gijbels 1996; Pagan and Ullah 1999; Yatchew 2003).

All the above models, other than the AR model, are nonlinear models. For Loess, Locpoly, and our model, the first-order (linear) prediction is utilized for all the numerical experiments.

In each experiment for each model, we produce 300 simulations. In each simulation, a time series with length 602 is generated from the synthetic model. We make the one-step and two-step predictions based on the first 600 data points and then calculate the three types of prediction errors by comparing with the observed values, that is, the last two generated data points. The mean, median, and standard deviation of the absolute prediction errors are computed over the 300 simulations for each type of prediction error. [The statistics are denoted by mean, median, std, respectively, in the tables of this section.] The mean squared prediction error (MSPE) for each type of prediction is also calculated.

The software for FAR was downloaded from <http://orfe.princeton.edu/~jqfan/fan/nls.html> (a supplement of Fan and Yao 2003). Implementation of TAR and AAR is based on an online software package that is downloadable at <http://cran.r-project.org/src/contrib/Descriptions/tsDyn.html> (Maintainer: Antonio, Fabio Di Narzo). Implementation of Locpoly is based on an online software package that is downloadable at <http://cran.r-project.org/src/contrib/Descriptions/JLLprod.html> (Maintainer: David Tomás, Jacho-Chávez). Implementation of AR can be found in the Matlab system identification toolbox; and Loess is implemented based on the function “loess” in the standard R package “stats.”

5.3.1 A Functional Coefficient Autoregressive Model

The first model (5.1) is an FAR model. The model is initialized with $X_0 = X_1 = X_2 = X_3 = 2$, and the first 100 data points form the warm-up period.

Table 1 shows that there is no significant difference between our method (HRM) and the method specific for FAR model. “1-s” stands for one-step prediction; “Ite” stands for iterative two-step prediction; “Dir” stands for direct two-step prediction. Among the nonlinear ones, FAR and our model give the most accurate prediction in this example. Linear AR model does not fit this nonlinear scheme well.

5.3.2 A Threshold Autoregressive Model

The second model is a TAR model,

$$X_t = \begin{cases} 0.62 + 1.25X_{t-1} - 0.43X_{t-2} + 0.3X_{t-3} - 0.2X_{t-4} + \varepsilon_t & \text{if } X_{t-2} \leq 2.25 \\ 2.25 + 1.52X_{t-1} - 1.24X_{t-2} - 1.25X_{t-3} + 0.4X_{t-4} + \varepsilon_t & \text{if } X_{t-2} > 2.25, \end{cases}$$

where $\{\varepsilon_t\}$ are iid from $N(0, 1.5^2)$. The model is initialized with $X_0 = X_1 = X_2 = X_3 = 0$, and the first 100 data points form the warm-up period.

Table 1. Prediction error under an FAR model.

	HRM			AAR(4)		FAR(4, 1)		
	1-s	Ite	Dir	1-s	Ite	1-s	Ite	Dir
Mean	0.16	0.18	0.18	0.19	0.20	0.16	0.17	0.20
Median	0.13	0.15	0.15	0.16	0.17	0.14	0.14	0.17
Std	0.12	0.13	0.14	0.15	0.15	0.12	0.13	0.15
MSPE	0.04	0.05	0.05	0.06	0.06	0.04	0.05	0.06
	AR(4)		Loess(4)		Locpoly(4)			
	1-s	Dir	1-s	Ite	1-s	Ite		
Mean	0.60	0.57	0.19	0.20	0.18	0.19		
Median	0.53	0.45	0.16	0.17	0.14	0.15		
Std	0.43	0.43	0.15	0.15	0.15	0.14		
MSPE	0.54	0.51	0.06	0.06	0.05	0.06		

From Table 2, we can see that TAR outperforms all the other methods. This is not surprising given the data generation mechanism. Because TAR may be considered as a special case of FAR, FAR(4, 2) is applied for the example. Our method performs similarly to AAR and FAR. Loess and Locpoly have the worst performance among the nonlinear methods. Once again the linear AR model does not fit the nonlinear situation well.

One possible reason for the underperformance of our method is the discontinuity of the underlying model on boundaries. Recall our method assumes that the underlying function f is differentiable, and we penalize on its Hessian. It will be interesting to further study the dependence of our method on the regularity of the underlying model.

Table 2. Prediction error for a TAR model.

	HRM			AAR(4)		TAR(4, 4; 2)			
	1-s	Ite	Dir	1-s	Ite	1-s	Ite		
Mean	1.42	2.30	2.31	1.39	2.30	1.25	2.14		
Median	1.10	1.87	1.94	1.10	1.85	1.03	1.72		
Std	1.32	1.90	1.95	1.27	1.84	1.00	1.55		
MSPE	3.75	8.89	9.15	3.55	8.63	2.59	6.98		
	FAR(4, 2)			AR(4)		Loess(4)		Locpoly(4)	
	1-s	Ite	Dir	1-s	Ite	1-s	Ite	1-s	Ite
Mean	1.45	2.43	2.48	3.76	6.08	2.16	4.45	1.69	2.49
Median	1.15	1.81	1.82	2.62	4.14	1.79	3.57	1.30	2.00
Std	1.23	2.01	2.38	4.07	6.79	1.72	3.36	1.53	2.07
MSPE	3.60	9.95	11.84	30.66	82.94	7.61	31.10	5.20	10.46

5.3.3 Other More Generic Models

The above two examples show that even when the data are generated from a perfect model (e.g., AAR, TAR, or FAR), our method still produces comparable prediction results with the original generating model.

The third model is

$$X_t = -X_{t-4} \exp(-2X_{t-3}^2) + \frac{1}{1 + 4X_{t-2}^2} \cos(1.5X_{t-1})X_{t-1} + \frac{X_{t-3}}{1 + 4X_{t-1}^2} + \frac{\exp(1.5(X_{t-4} - 1))}{1 + \exp(1.5(X_{t-4} - 1))} + \varepsilon_t, \quad (5.2)$$

where $\{\varepsilon_t\}$ are iid from $N(0, 0.5^2)$. The model is initialized with $X_j \sim N(0, 0.2^2)$, where $j = 0, \dots, 3$, and the first 100 data points are the warm-up period. The fourth model is

$$X_t = [0.2 + (0.3 + X_{t-3}) \exp(-4X_{t-4}^2)]X_{t-1} + [-0.4 - (0.7 + 1.3X_{t-3}) \exp(-4X_{t-4}^2)]X_{t-2} + \varepsilon_t, \quad (5.3)$$

where $\{\varepsilon_t\}$ are iid from $N(0, 0.5^2)$. The model is initialized with $X_j \sim N(0, 1)$, where $j = 0, \dots, 3$, and the first 100 data points belong to the warm-up period.

The above two examples are nonlinear and cannot be characterized by AAR, FAR, or TAR. Table 3 demonstrates that our method outperforms all three methods in both one-step and iterative two-step predictions.

Loess, Locpoly, and our method are all nonlinear models and do not require any specific model structure. Although all three methods are local approaches, the great advantage of our method is that the penalty term of the Hessian functional can also take into account the global properties of the data. For the above four examples, Loess always has the worst performance among the three. Occasionally, our method and Locpoly have comparable performance, for example, for the one-step prediction in the third example, but our method often outperforms Locpoly, for example, in the first two examples.

The third and fourth examples illustrate the flexibility of our method, because our method does not enforce any specific structure on the model. In some cases when the data are not generated from a perfect model, for example, AAR, TAR, or FAR, our method can generate a more accurate prediction than other methods.

5.4 REAL DATASETS

Here we apply HRM to some well-studied datasets and comparison with other reported works is made. In many cases, our model outperforms methods that are used by other researchers.

5.4.1 Sunspot Data

Sunspot data are well studied in the literature (Chen and Tsay 1993; Fan and Yao 2003 and many more). The data are downloadable from the web site of Fan and Yao (2003). Table 8.5 in the work of Fan and Yao (2003) summarizes results for several previous models, including:

Table 3. Prediction error under two nonlinear models.

(a) Under model (5.2)												
	HRM			AAR(4)		AR(4)		Loess(4)		Locpoly(4)		
	1-s	Ite	Dir	1-s	Ite	1-s	Dir	1-s	Ite	1-s	Ite	
Mean	0.47	0.56	0.56	0.52	0.64	0.95	0.89	0.58	0.62	0.46	0.59	
Median	0.39	0.41	0.43	0.44	0.53	0.82	0.76	0.47	0.50	0.38	0.44	
Std	0.35	0.55	0.52	0.40	0.58	0.73	0.69	0.45	0.56	0.35	0.56	
MSPE	0.34	0.62	0.58	0.43	0.74	1.43	1.26	0.54	0.70	0.33	0.66	
	FAR(4, 1)			FAR(4, 2)			FAR(4, 3)			FAR(4, 4)		
	1-s	Ite	Dir	1-s	Ite	Dir	1-s	Ite	Dir	1-s	Ite	Dir
Mean	0.51	1.00	0.62	0.59	0.97	0.63	0.56	1.03	0.58	0.57	1.00	0.59
Median	0.41	0.82	0.48	0.49	0.81	0.51	0.44	0.92	0.46	0.45	0.81	0.48
Std	0.39	0.78	0.63	0.47	0.77	0.53	0.55	0.77	0.50	0.45	0.75	0.55
MSPE	0.42	1.61	0.79	0.57	1.54	0.67	0.62	1.66	0.58	0.53	1.56	0.65
(b) Under model (5.3)												
	HRM			AAR(4)		AR(4)		Loess(4)		Locpoly(4)		
	1-s	Ite	Dir	1-s	Ite	1-s	Dir	1-s	Ite	1-s	Ite	
Mean	0.52	0.49	0.52	0.65	0.53	0.82	0.71	1.53	1.12	0.52	0.48	
Median	0.40	0.37	0.36	0.48	0.39	0.57	0.52	0.61	0.54	0.40	0.38	
Std	0.81	0.50	0.74	1.08	0.52	1.08	0.69	5.71	2.71	0.90	0.45	
MSPE	0.92	0.48	0.82	1.59	0.54	1.85	0.97	34.85	8.54	1.09	0.43	
	FAR(4, 1)			FAR(4, 2)			FAR(4, 3)			FAR(4, 4)		
	1-s	Ite	Dir	1-s	Ite	Dir	1-s	Ite	Dir	1-s	Ite	Dir
Mean	0.64	0.61	0.62	0.80	0.56	0.52	0.61	0.54	0.60	0.67	0.58	0.56
Median	0.47	0.43	0.42	0.46	0.39	0.40	0.44	0.41	0.42	0.48	0.42	0.38
Std	1.00	0.94	0.98	3.33	0.80	0.55	0.89	0.60	0.65	1.10	0.60	0.63
MSPE	1.42	1.25	1.35	11.69	0.94	0.57	1.16	0.65	0.77	1.65	0.70	0.71

- FAR-1, a functional coefficient autoregressive model fitted via local polynomial methods, as specified by (8.19) together with figure 8.5 in the book by Fan and Yao (2003);
- FAR-2, a functional coefficient autoregressive model fitted by Chen and Tsay (1993), with exact formula given in (8.18) in the book by Fan and Yao (2003);
- TAR, a threshold autoregressive model that is specified in (8.20) in the book by Fan and Yao (2003).

In all the above models the number of lags is $p = 8$. In our model we chose $p = 6$. (We chose $p = 6$ because the GCV and prediction errors are stabilized at this point.) The number of nearest neighbors ($k = 29$) is chosen by minimizing the aforementioned function $GCV(\cdot)$, which is a function of both λ and k .

Table 4. Prediction errors for sunspot data.

Year	HRM		FAR-1		FAR-2		TAR	
	1-s	Itc	1-s	Itc	1-s	Itc	1-s	Itc
1980	1.5	1.5	1.4	1.4	13.8	13.8	5.5	5.5
1981	7.8	9.1	11.4	10.4	0.0	3.8	1.3	0.0
1982	9.6	14.1	15.7	20.7	10.0	16.4	19.5	22.1
1983	8.1	4.0	10.3	0.7	3.3	0.8	4.8	6.5
1984	3.3	1.0	1.0	1.5	3.8	5.6	14.8	15.9
1985	10.3	8.1	2.6	3.4	4.6	1.7	0.2	2.7
1986	0.4	7.3	3.1	0.7	1.3	2.5	5.5	5.4
1987	9.5	9.1	12.3	13.1	21.7	23.6	0.7	17.5
AAPE	6.3	6.8	7.2	6.5	7.3	8.3	6.6	9.5

Table 4 presents the prediction errors of our method (column HRM) together with errors from the above three methods (copied from [Fan and Yao 2003](#), table 8.5). Our method generates the smallest one-step average absolute prediction error. Our average absolute prediction error of two-step prediction is slightly worse than that of FAR-1. However, we still outperform FAR-2 and TAR. Note that the above is achieved by using six (instead of eight) predictors in our method.

5.4.2 Blowfly Data

We apply our method to the blowfly data (downloadable at www.robjhyndman.com/TSDL/ecology.html). It is known that the first 206 data points are nonlinear and the remaining data points are almost linear ([Tsay 1988](#)). Thus we use the first 195 data points as training data, then make postsample prediction for data points 196 to 210. Log-transformation is taken on the blowfly data in accordance with the literature. To get rid of the round-off error from calculating the optimal λ for GCV in our method, we multiply the log data by 10.

Four other models are compared. A threshold autoregressive model TAR(1, 3; 8) is suggested by [Tong \(1990, p. 337\)](#). We apply the model with the same order but refit the model (column TAR), because the original model is applied to a different segment of the time series. To verify the order of the TAR model for our training data, we automatically select the best order of the TAR model with respect to the pooled AIC criteria, using the “select-SETAR” procedure in R package “tsDyn.” Fixing the threshold variable as the eighth lag, TAR(2, 3; 8) is selected. Because the second variable in the lower regime is not significant, TAR(1, 3; 8) is nearly identical with TAR(2, 3; 8).

The second and third models are functional coefficient autoregressive (FAR) models with different number of dependent variables:

- FAR-1: $X_t = f_0(X_{t-8}) + f_1(X_{t-8})X_{t-1} + f_2(X_{t-8})X_{t-2} + f_3(X_{t-8})X_{t-3} + \varepsilon_t$,
- FAR-2: $X_t = f_0(X_{t-8}) + f_1(X_{t-8})X_{t-1} + f_2(X_{t-8})X_{t-2} + f_3(X_{t-8})X_{t-3} + f_4(X_{t-8})X_{t-4} + \varepsilon_t$.

Table 5. Prediction errors for blowfly data.

Obs.	HRM		TAR(1, 3; 8)		FAR-1		FAR-2		AR(8)	
	1-s	Ite	1-s	Ite	1-s	Ite	1-s	Ite	1-s	Ite
196	0.040	0.196	0.048	0.175	0.112	0.236	0.089	0.227	0.003	0.266
197	0.052	0.008	0.035	0.031	0.012	0.174	0.009	0.139	0.075	0.144
198	0.004	0.076	0.014	0.033	0.062	0.081	0.057	0.071	0.087	0.078
199	0.010	0.003	0.015	0.035	0.029	0.125	0.023	0.113	0.031	0.117
200	0.078	0.061	0.092	0.113	0.097	0.142	0.090	0.126	0.066	0.033
201	0.136	0.261	0.163	0.290	0.129	0.266	0.138	0.257	0.271	0.241
202	0.049	0.240	0.063	0.287	0.060	0.215	0.071	0.232	0.322	0.410
203	0.000	0.040	0.081	0.004	0.045	0.024	0.047	0.033	0.121	0.442
204	0.108	0.107	0.071	0.040	0.082	0.032	0.063	0.011	0.051	0.416
205	0.046	0.158	0.036	0.134	0.031	0.114	0.012	0.077	0.088	0.199
206	0.180	0.130	0.175	0.124	0.177	0.146	0.159	0.147	0.208	0.167
207	0.234	0.016	0.298	0.059	0.186	0.018	0.192	0.038	0.040	0.039
208	0.007	0.286	0.033	0.441	0.028	0.176	0.019	0.190	0.210	0.078
209	0.081	0.090	0.107	0.061	0.099	0.139	0.055	0.081	0.167	0.174
210	0.111	0.210	0.154	0.301	0.134	0.290	0.148	0.235	0.350	0.114
Ave.	0.076	0.126	0.092	0.142	0.086	0.145	0.078	0.132	0.139	0.195

A similar model with two dependent variables is given by [Xia and Li \(1999\)](#). Note that the above FAR-1 model corresponds to the TAR model in the book by [Tong \(1990\)](#). Moreover, we observe that more dependent variables can dramatically reduce the prediction errors of the FAR model for our training data. The fourth model is a standard autoregressive model with eight lags.

To compare, we fit a generic model, $X_t = f(X_{t-1}, X_{t-2}, X_{t-3}, X_{t-4}, X_{t-8}) + \varepsilon$, via HRM. We choose this form because it corresponds to FAR-2, which gives the best numerical performance in this dataset. The number of the nearest neighbors ($k = 21$) is chosen by GCV.

The results are reported in Table 5. It is observed that when our model is applied, both the average one-step prediction error and the average two-step prediction error are smaller than those of the four competing methods. This example once again demonstrates the advantage of HRM.

6. DISCUSSION AND CONCLUSION

We introduce a Hessian regularized nonlinear time series model for prediction in time series. The approach is especially powerful when the number of dependent variables is greater than three, which cannot be handled by natural cubic splines and thin-plate splines. Moreover, our approach is nonlinear and nonparametric and does not enforce any specific structure on the model. Both theoretical and simulation results provide strong verification and support of our approach.

Other penalty forms are possible. One alternative penalty is the Laplacian:

$$\mathcal{L}f = \int_{\Omega} \sum_i |f_{ii}(\mathbf{z})|^2 d\mathbf{z}.$$

The difference between the Hessian ($\mathcal{H}f$) and Laplacian ($\mathcal{L}f$) is that the latter does not consider the cross-terms. It is known that $\mathcal{H}f$ is translation and rotation invariant, whereas $\mathcal{L}f$ is not. Hence, we prefer the Hessian. Another interesting alternative is to consider a modified function:

$$\int_{\Omega} \sum_{i,j} |f_{ij}(\mathbf{z})| d\mathbf{z}. \quad (6.1)$$

Note the above penalty function uses sum of absolute values, instead of sum of squares. Penalty function (6.1) may have some nice properties. However, it is known that minimizing the sum of absolute values (i.e., the ℓ_1 norm) is much more computationally demanding than minimizing the sum of squares (i.e., the ℓ_2 norm). A penalty function like (6.1) has been explored in trigrams (Koenker and Mizera 2004).

More technical discussion, such as the possibility of fast computing and speculation on a formal proof of convergence, can be found in an online technical report (Chen and Huo 2007). Software related to this paper is available at www.isye.gatech.edu/~xiaoming/software/. Readers can also refer to the supplementary materials of this paper.

SUPPLEMENTAL MATERIALS

HRM Software: The archive contains Matlab and R code to perform the experiments described in the article and the datasets used as examples. An .htm file is written as a user-friendly interface—readers are recommended to open this file first using any web browser. (hrm2009-web-based-software.tar.gz, GNU zipped tar file)

ACKNOWLEDGMENT

This work has been partially supported by National Science Foundation grants DMS 0604736 and 0700152.

[Received April 2008. Revised June 2009.]

REFERENCES

- Cai, Z., Fan, J., and Yao, Q. (2000), "Functional-Coefficient Regression Models for Nonlinear Time Series Models," *Journal of the American Statistical Association*, 95, 941–956.
- Chen, J. (2007), "Theoretical Results and Applications Related to Dimension Reduction," Ph.D. thesis, Georgia Institute of Technology, available at etd.gatech.edu.
- Chen, J., and Huo, X. (2007), "A Hessian Regularized Nonlinear Time Series Model," technical report, Georgia Institute of Technology, available at www2.isye.gatech.edu/statistics/papers/08-01.pdf.
- Chen, R., and Tsay, R. S. (1993), "Functional-Coefficient Autoregressive Models," *Journal of the American Statistical Association*, 88, 298–308.

- Cleveland, W. S. (1979), "Robust Locally Weighted Regression and Smoothing Scatterplots," *Journal of the American Statistical Association*, 74, 829–836.
- (1988), "Locally Weighted Regression: An Approach to Regression Analysis by Local Fitting," *Journal of the American Statistical Association*, 83, 596–610.
- Fan, J., and Gijbels, I. (1996), *Local Polynomial Modelling and Its Applications*. Monographs on Statistics and Applied Probability, Vol. 66, New York: Chapman & Hall.
- Fan, J., and Yao, Q. (2003), *Nonlinear Time Series: Nonparametric and Parametric Methods*, New York: Springer.
- Fan, J., Yao, Q., and Cai, Z. (2003), "Adaptive Varying-Coefficient Linear Models," *Journal of the Royal Statistical Society, Ser. B*, 65, 57–80.
- Green, P. J., and Silverman, B. W. (1994), *Nonparametric Regression and Generalized Linear Models: A Roughness Penalty Approach*. Monographs on Statistics and Applied Probability, Vol. 58, New York: Chapman & Hall.
- Hastie, T. J., and Tibshirani, R. J. (1990), *Generalized Additive Models*. Monographs on Statistics and Applied Probability, Vol. 43, New York: Chapman & Hall.
- Johnstone, I. M. (2004), "Function Estimation and Gaussian Sequence Models," unpublished monograph, available at www-stat.stanford.edu/~imj/baseb.pdf.
- Koenker, R., and Mizera, I. (2004), "Penalized Triograms: Total Variation Regularization for Bivariate Smoothing," *Journal of the Royal Statistical Society, Ser. B*, 66, 145–163.
- Pagan, A., and Ullah, A. (1999), *Nonparametric Econometrics*, New York: Cambridge University Press.
- Tong, H. (1990), *Nonlinear Time Series: A Dynamical System Approach*, New York: Oxford University Press.
- Tsay, R. S. (1988), "Non-Linear Time Series Analysis of Blowfly Population," *Journal of Time Series Analysis*, 9, 247–264.
- Wahba, G. (1990), *Spline Models for Observational Data*. CBMS-NSF Regional Conference Series in Applied Mathematics, Philadelphia, PA: Society for Industrial and Applied Mathematics.
- Xia, Y., and Li, W. K. (1999), "On the Estimation and Testing of Functional-Coefficient Linear Models," *Statistica Sinica*, 9, 735–757.
- Yatchew, A. (2003), *Semiparametric Regression for the Applied Econometrician*, New York: Cambridge University Press.